

**CHARACTERIZING THE IMMUNE PHENOTYPE OF  
TUMOR INFILTRATING LYMPHOCYTES IN RENAL  
CELL CARCINOMA**

A THESIS PRESENTED  
BY  
MOON HEE LEE  
TO  
THE FACULTY OF MEDICINE

IN PARTIAL FULFILLMENT OF THE REQUIREMENTS  
FOR THE DEGREE OF  
MASTER OF SCIENCE  
IN THE SUBJECT OF  
TRANSLATIONAL MEDICINE

UNIVERSITY OF HELSINKI  
HELSINKI, FINLAND  
MAY 2017

©2017 – MOON HEE LEE  
ALL RIGHTS RESERVED

University of Helsinki, Faculty of Medicine, School of Medicine  
International Master's Degree Program in Translational Medicine  
Moon Hee Lee: *Characterizing the Immune Phenotype of Tumor Infiltrating Lymphocytes in Renal Cell Carcinoma*  
Master of Science Thesis; 37 pages  
Supervisors: Anna Kreutzman PhD<sup>1</sup>, Satu Mustjoki MD, PhD<sup>1</sup>  
<sup>1</sup>Hematology Research Unit Helsinki, University of Helsinki and Helsinki University Hospital Comprehensive Cancer Center  
03. 05. 2017

**Keywords:** renal cell carcinoma, RCC, NK cell, immune checkpoint, tumor infiltrating lymphocytes, TILs

## Abstract

Cancer immunotherapy has advanced with the introduction of anti-PD-1 therapy. Anti-PD-1 therapy blocks the inhibitory immune checkpoint receptor PD-1, and allows T cells to regain their cytotoxic potentials in response to cancerous cells. Amongst the cytotoxic lymphocytes other than T cells, natural killer (NK) cells have not been fully explored regarding anti-PD-1 treatment. With this in mind, our aim was to characterize the immunophenotype of the immune cells in patients diagnosed with renal cell carcinoma (RCC), and separate their corresponding tumor infiltrating lymphocytes (TILs).

Altogether, we analyzed the immunophenotype of the T and NK cells and RCC tumor cells from 13 RCC patients using flow cytometry. In addition, we tested the function of NK cells against RCC cells using various cell line models (NK-92 and RCC cell lines), and monitored the cytotoxicity in real time using a cell impedance assay. Based on the results, we suggest that patients diagnosed with RCC possess unique immune profiles depending on the individual, but also share characteristics regarding the tumor. In addition, NK cells have the potential to activate a cytotoxic response to RCC cells. By phenotyping the TILs, potential novel biomarkers for immuno-oncological (IO) therapy could be detected, which could aid in determining which patients would most likely benefit from immunological therapies such as anti-PD-1 treatment.

# Contents

Introduction	1
Materials and Methods	4
Results	12
Discussion	23
References	28

## Acknowledgments

Firstly, I would like to give thanks and praise to the Lord, my God, for the strength and unconditional love thus far in my life. I would like to express my gratitude to my supervisors Anna Kreutzman and Professor Satu Mustjoki for planning the project and providing their support and perseverance in making this thesis possible. Furthermore, I would also like to thank Anna Kreutzman and Henna Hakanen for their patience and guidance through the practical work during the project. Their words of encouragement and wicked sense of humor kept me going through thick and thin. Lastly, I would like to express my gratitude to my parents and brother for encouraging me through tears and laughter as well as giving me endless spiritual support.



## Introduction

Among the most common cancer killers in men and women, kidney cancer is within the top 10, with a lifetime risk of about 1 in 63 (1.6%) for development<sup>1</sup>. The incidence of kidney cancer, especially among the elderly, is on the rise with approximately 908 new cases per year and 362 deaths (incidence 2010-2014) are seen annually in Finland<sup>2</sup>. Although multiple therapies that target tumor growth and angiogenesis are effective, they fail at keeping the tumors from returning. In adults, clear cell renal cell carcinoma (ccRCC) is the most dominant type of the cancer. Early stages of the cancer show hardly noticeable symptoms. When symptoms are detected, it is most likely that the cancer has metastasized and reached the advanced phase of the disease. Despite the numerous options of treatment other than surgery (nephrectomy is surgical procedure of choice), kidney cancer remains difficult to treat, thus is yet poorly understood.

With a current wide variety of chemotherapeutic drugs, only a handful has shown responses in RCC. This may be due to the fact that RCC is mostly resistant to radio and chemotherapies. Another alternative would be to harness the immune system in treating cancer. Initially, cytokine-based immune therapies such as interleukin 2 (IL-2) and interferon  $\alpha$  (IFN $\alpha$ ) have shown to be effective in RCC. However, the suitability of these treatments has not been proven ideal due to the toxic adverse effects from the use of high IL-2 concentrations, and the ineffectiveness of IFN $\alpha$  monotherapy<sup>3</sup>. Today, a more powerful generation of targeted immune therapies are on the rise, namely immune checkpoint inhibitors, which are antibodies designed to counteract the molecular pathways that the tumor cells participate in evading immune recognition.

Immune checkpoints are a necessity to the human immune system and are responsible for maintaining self-tolerance or the prevention of autoimmunity, as well as the protection of tissues against damage in response to pathogenic infections. However, the expression of these immune checkpoint proteins may become dysfunctional when they act as an immune resistance mechanism from the attack of tumors. Although the human immune system has capabilities of targeting and eliminating cancer cells, a fraction of these cancer cells has the ability to escape the body's immunosurveillance by forming tumors and further, metastases. One form of escape is the ability of some tumor types to express ligands that inhibit the activation of tumor-specific lymphocytes<sup>4</sup>. The majority of these ligands are those that interact with the immune checkpoint pathways responsible for the inhibition of immune system signals. Blocking immune checkpoints is a competent approach to cancer therapy today. In the case of stage IV melanoma, the drugs nivolumab (Opdivo<sup>®</sup> BMS) and

pembrolizumab (KEYTRUDA<sup>®</sup>, Merck) have been approved in the EU and Finland, functioning as immune checkpoint inhibitors that act to block the inhibition pathway of T cell activation. Their mechanism of action is based on inhibiting the programmed death protein 1 (PD-1) from binding to its ligand, programmed death receptor ligand 1 (PD-L1) in the form of monoclonal antibodies (mAbs). The PD-1 receptor is widely expressed on the surface of activated T cells and functions as a negative regulator of T cell activation. In addition to antigen presenting cells (APCs), tumor cells are also able to express PD-L1 and PD-L2 that bind to the PD-1 receptor and inactivate the immune system<sup>4</sup>. From the initial anti-PD-1 treatment in melanoma patients, similar regimens have been applied to RCC patients, and further, to a broader spectrum of immune checkpoint therapies. With this in mind, it is noticeable that PD-1 inhibitors have already been approved in the United States and Europe for the treatment of advanced RCC patients, under various stages of clinical development<sup>5,6</sup>.

The human immune system is classified into the adaptive and innate subsystems. The adaptive system is responsible for a highly controlled and long-lasting response, and the innate for a rapid and unspecific immune response, as well as inducing the functioning of the adaptive immune system at the site of action. T cells are major players of the adaptive immune system. Furthermore, their lymphocytic division into cytotoxic CD8<sup>+</sup> effectors and CD4<sup>+</sup> helpers make T cells critical to the adaptive and innate immune systems. Due to their potential in selectively recognizing peptides derived from all proteins of the cellular compartment, T cells show great promise in becoming manipulated for antitumor immunity. Their mechanism of action entails the interaction between the T cell receptor (TCR) and the pathogenic tumor antigens presented by the major histocompatibility complex (MHC) molecules. The engagement of the TCR with the MHC then activates a series of signal transduction events that lead to antitumor immunity and activation of the intracellular cytotoxic machinery that recognizes and kills that target cancer cells<sup>3</sup>. The use of one's own immune system in the treatment of cancer and the usage of immune checkpoints offer a great capacity to initiate an antitumor immune response, and thus also pave a new way for future cancer therapies<sup>7</sup>.

Natural Killer (NK) cells belong to the family of cytotoxic lymphocytes that are part of the innate immune system and have the ability to spontaneously kill cells that are deemed harmful to the host. NK cells are able to migrate, produce and secrete lymphocyte-stimulating cytokines at the site of action, acting to protect and guide the immune system<sup>8</sup>. The cells are able to kill their targets without requiring the recognition of the MHC presented on cell surfaces<sup>9</sup>. Based on their functional characterization, NK cells are vital in the prohibition of tumor growth as well as metastases. However, malignant cells are still able to surpass this checkpoint from the lack in number of NK cells, as well as impairments in their inhibition abilities, and decrease in cell signal activation. NK cell activation occurs through a crosstalk



of activating and inhibitory signals that are received on the NK cells. Inhibitory ligands such as PD-L1 expressed on the surface of the target tumor cells or APCs prevent NK cells from activating<sup>4</sup>. Therefore, trying to eliminate these signals via the blocking of mAbs such as PD-1 would restore NK cell activity and function. Currently, immune checkpoints are less studied in regard to their function in NK cells. However, it is certain that NK cells are essential in responding to various types of cancers and therapeutics so that their functions may be improved. One successful case would be the combinatorial treatment of relapsed acute myeloid leukemia patients (AML) with the anti-killer-cell immunoglobulin-like receptor (KIR) mAb (Lirilumab<sup>®</sup> BMS), which inhibits the KIR2DL-1, -2 and -3 inhibitory receptors and their ligands, resulting in activated NK cells<sup>10</sup>.

The objective of this study was to characterize the phenotype of intratumoral immune cells (tumor infiltrating lymphocytes; TILs) in RCC tumors derived from patients diagnosed with kidney cancer. Upon receiving freshly excised patient RCC tumors from nephrectomies, the samples were used for the immunophenotyping of the TILs. Also, we aimed to use *in vitro* methods to investigate the function of NK cells against RCC cell lines. The cells were further assessed using a real time killing assay for functional analyses of the cells.

From our results, we have identified different immune profiles of the TILs, as well as observed the expression markers concerning the immune phenotype of RCC tumor cells. The characterization patterns of the cell populations expressing T, NK and tumor specific markers were analyzed, providing an immune profile regarding each RCC patient. Based on the results, we suggest that patients diagnosed with RCC possess unique immune profiles depending on the individual, but also share characteristics regarding the tumor. In addition, we have tested the functional aspects of RCC cancer cells *in vitro* by testing their cytotoxic abilities. From our results, we have concluded that NK cells have the potential to activate a cytotoxic response to RCC cells.

## Materials and Methods

### **Patients and samples**

The ongoing study included 13 RCC patients that underwent a surgical removal of the tumors, mostly via partial, or in some cases, radical nephrectomy. Tumor samples were collected and delivered directly from the University of Helsinki Hospital Comprehensive Cancer Center as well as from Peijas Hospital (Vantaa), as soon as the patient's blood circulation was closed off. Physicians Harry Nisen and Petrus Järvinen were responsible in kindly providing us with the patient samples.

### **Ethical considerations**

The approval for laboratory studies, collection of peripheral blood, tumor biopsies and RCC tumor samples has been obtained from the HUCH ethical committee (115/13/03/02/15). All patients gave a written informed consent and the study was approved by the local university hospitals (Meilahti and Peijas). In addition, the permission to perform the studies has been secured from the University of Helsinki Comprehensive Cancer Hospital. Subject anonymity has been guaranteed whereby each patient was given a number code for further use in the laboratory.

### **Storage and handling of RCC tumor samples**

Each RCC tumor sample was collected in 50mL Falcon tubes containing 10 - 15mL MACS Tissue Storage Solution (Miltenyi Biotec). The sample was first weighed and photographed to measure the size and morphology. The tumors were then minced and homogenized according to Miltenyi's Tumor Dissociation Kit protocol. After the tumors were homogenized, the viable cells were counted with the Sysmex XP-300<sup>TM</sup> automated hematology analyzer. After resuspending the sample in 1 x PBS, 500 $\mu$ L of the tumor cells were set aside for flow cytometric analysis. In total, four pellets between  $1 - 10^7$  (depending on the total cell count) cells were frozen in  $-70^{\circ}\text{C}$ , whereby two were stored in the RNALater Solution (Invitrogen) and the other two frozen as pellets. The rest of the cells were live frozen in fetal bovine serum (FBS; Gibco) + 10% DMSO in  $5^6 - 10^8$  aliquots for later experiments.

### **Miltenyi Biotec tumor dissociation kit**

Tumors were dissociated into single-cell suspensions by mechanical and enzymatic digestion of the extracellular matrix. The gentleMACS™ Dissociator instrument was utilized for the mechanical degradation procedures (program for soft tumors). After the dissociation, the samples were applied to a filter to remove any larger particles from the single-cell suspensions and were resuspended in RPMI 1640 (LONZA) until further processing. The tumor cells were immediately processed for phenotyping the tumor cell population and downstream applications. The kit is designed for a simple yet effective generation of single-cell suspensions using primary human tumor tissue.

### **Multicellular tumor spheroids**

Solid, 3D tumor spheroids were generated using the A-498 and CAKI-1 RCC cell lines by seeding 3 cells/100uL per well in a volume of 100uL/well of culture medium in 96-well ultra-low cluster, 96-well round bottom plates (Corning). The growth was monitored every two days after the third day of initial seeding (d0, d3, d5, d7...d30). The growth of the spheroids was monitored under a phase contrast microscope (Biorad) and imaged. The spheroids were left to grow until the diameters reached between 400 – 700µm in size.

### **Cell culture**

Human renal cell carcinoma cell lines CAKI-1, CAKI-2, A498 were cultured in their corresponding media 80% McCoy's 5a + 20% h.i. fetal bovine serum (FBS) for CAKI-1, CAKI-2, and 90% MEM (with Earle's salts) + 10% FBS for A-498, respectively. The cytotoxic lymphocyte cell line, NK-92 was cultured in RPMI 1640 (LONZA) + 10ng/mL IL-2. In addition, all the media were supplemented with 10% FBS 1% L-Glutamine (LONZA), 1% Penicillin-Streptomycin (LONZA) and the cell lines were cultured at 37°C in 5% CO<sub>2</sub>. The human kidney carcinoma cell lines CAKI-1, CAKI-2 and A-498 were ordered from DSMZ, Germany, DSMZ no. ACC 731, ACC 54, and ACC 55, respectively. The cytotoxic NK-92 cell line was also ordered from DSMZ, Germany, DSMZ no. ACC 488.

In addition, we used two human renal cell adenocarcinoma cell lines AHCN and 786-O, kindly provided by Piia Mikkonen and Vilja Pietiäinen (Kallioniemi group, Institute of Molecular Medicine Finland (FIMM)). Both cell lines were cultured in RPMI 1640 (LONZA) media supplemented with 10% FBS, 1% L-Glutamine, 1% Penicillin-Streptomycin, at 37°C and 5% CO<sub>2</sub>.

## Immunophenotyping of RCC tumors

The RCC patient tumor samples were analyzed by an immunophenotyping assay using flow cytometry (BD FACS Verse) with a panel of fluorescently labeled antibodies that were specifically selected in order to characterize the phenotype of the NK, T, and tumor cells. The immunophenotyping antibody panel consisted of four tubes with specific antibodies and one unstained control (Table 1). All the antibodies were titrated in order to obtain the optimal volumes for their usage in the phenotyping assay (the volumes in  $\mu\text{L}$  for each antibody are presented in Table 1). For each tube, the antibodies and  $100\mu\text{L}$  of the dissociated tumor sample were added. Then, the tubes were incubated in the dark for 15min at room temperature. After the incubation, the cells washed three times with 1mL of 1 x PBS via centrifugation ( $300g \times 5 \text{ min}$ ), and resuspended in  $300\mu\text{L}$  of 1 x PBS for analysis. The FACS Suite software was set to acquire  $1 \times 10^6$  total events from each tube.

**Table 1 | Immunophenotyping panel**

All tubes contain antibodies to detect the main lymphocyte subpopulations (CD45 for lymphocytes, CD3 for T cells and CD56 for NK cells). **Tube B1** Contains the immune checkpoint inhibitors PD-1 and LAG-3. PD-L1 and PD-L2 were also included to observe how much of the ligands were expressed in the RCC tumors. **Tube B2** The CXC chemokine receptors CXCR3 and CXCR4 are markers were selected to observe the regulation and migratory behavior of the T and NK cells. The NK-specific marker CD16 is associated with antibody dependent cellular cytotoxicity (ADCC). **Tube B3** The NKG2 family of proteins is mostly expressed on the surface of naïve NK cells responsible for the NK cell activation, and DNAM-1 (CD226) indicates NK cell maturation. **Tube B4** c-Met and cytokeratin are markers targeting tumor cells. 7-AAD was included as a common cell viability marker.

<b>Tube B1</b>	1	BB515	PD1	2.5	<b>Tube B2</b>	1	FITC	CXCR3	10
	2	PE	LAG-3	5		2	PE	CD16	1
	3	PerCP-Cy5.5	CD3	5		3	PerCP-Cy5.5	CD3	5
	4	PE-Cy7	PDL1	10		4	PE-Cy7	CD4	1
	5	APC	PDL2	10		5	APC	CXCR4	2.5
	6	APC-H7	CD45	1		6	APC-H7	CD45	1
	7	BV510	CD8	1		7	BV510	CD8	1
	8	BV421	CD56	2.5		8	BV421	CD56	2.5
<b>Tube B3</b>	1	BB515	DNAM	1	<b>Tube B4</b>	1	BB515	CD13	5
	2	PE	CD57	2.5		2	PE	CD31	5
	3	PerCP-Cy5.5	CD3	5		3	PerCP-Cy5.5	7AAD	10
	4	PE-Cy7	NKG2D	1		4	PE-Cy7	CD3	2
	5	APC/AlexaFluor647	NKG2A	5		5	AF647	c-MET	5
	6	APC-H7	CD45	1		6	APC-H7	CD45	1
	7	BV510	CD8	1		7	BV510	Cytokeratin	5
	8	BV421	CD56	2.5		8	BV421	CD56	2.5

### Real-time cell impedance and cytotoxicity assay

The iCelligence™ instrument monitors the electrical impedance in a noninvasive manner to quantify the proliferation, morphology change, and attachment quality of cells in a label-free, real-time condition. The killing assay (real-time) was initially performed using, human renal cell carcinoma and later, renal cell adenocarcinoma cell lines. The A-498, CAKI-1, CAKI-2 (carcinoma), and AHCN, 786-O (adenocarcinoma) lines were used as targets to see the cytotoxic effects of the effector NK-92 cells.

In the assay, the cellular impedance (CI) of the adherent target cells growing at the bottom of the RTCA iCelligence™ (ACEA Biosciences, Inc) plates was measured. In this system, cellular growth and proliferation corresponds to an increase in the CI, whereas a decrease in CI would signify cell death and/or detachment from the plates.

The killing assay was initiated by resetting the instrument (executing one sweep with 395µL of the corresponding cell line media). Two sessions (first target, later target and effector cells), each with 1440 total sweeps per minute for a total of 24h was measured (Table 2). After reset, 50 000 adherent target cells x 8 wells / plate were seeded (5µL of 10<sup>7</sup>/ mL cell suspension) via reverse pipetting, totaling a volume of 395uL in each of the wells. The target cells were cultured for 24h at 37°C in 5% CO<sub>2</sub> to obtain fully confluent wells. After 24h, 200µL of the old media was removed from the wells. The effector cells were then added according to the effector to target (E:T) ratio (Table 3), and the total volume re-adjusted to 400µL by adding the appropriate volume of fresh cell media. The effectors and targets were co-cultured for 24h, in which the target CI was measured every minute.

**Table 2 | iCelligence killing assay in real-time**

Step	Sweeps	Duration	Interval
Reset	1/1	1min	1min
Target Cells	1440/1440	24h	1min
Target-Effector	1440/1440	24h	1min

The iCelligence instrument was reset before seeding the target cells. After system reset, the target cells were seeded and the impedance measured every minute for 24h to obtain a confluent monolayer of cells. On the following day, the effector cells were added to the wells and were co-incubated for 24h, with the impedance being measured every minute.

First, a dose-response with NK-92 effector cells against the A-498, AHCN, CAKI-1, CAKI-2 and 786-O cell lines as the target cells were measured to test the suitability of NK-mediated cell killing. The NK-92 cell line is known to have cytotoxic features and originates from a rare NK-cell lymphoma patient that enables the NK cells to grow continuously<sup>11</sup>. The E:T ratios (Table 3) were obtained from the literature<sup>12</sup>

**Table 3 | Effector to target ratios used in the killing assay**

Effector to target (E:T) ratios used in the direct killing assays  
Target cells tested: A-498, CAKI-1, CAKI-2, AHCN, 786-O  
Effector cells: NK-92

	<b>Target</b>	<b>Effector</b>
Target control	50 000	50 000
Effector control	50 000	50 000
4:1	200 000:50 000	200 000:50 000
8:1	400 000:50 000	400 000:50 000
16:1	800 000:50 000	800 000:50 000

\*The E:T ratios were carried out in duplicates to ensure consistency of the results

### **iCelligence™ functional assay**

The cellular impedance (CI) from the iCelligence assay was analyzed using the RTCA iCelligence Software (ACEA Biosciences). The impedance curve was first normalized to the last measured impedance of the cultured target cells before the addition of the effectors. The cytotoxic activity percentage after the 24h of co-incubation at a given effector to target (E:T) ratio was counted in Excel by the following equation<sup>13</sup>:

$$\text{Cytotoxic Activity \%} = (1 - CI_{24hE:T} / CI_{24h\text{ control}}) \times 100$$

After normalizing and counting the cytotoxic activity percentage, the data was converted to a CSV file and uploaded to Prism GraphPad for statistical analysis and graphing.

### **Data analysis**

The immunophenotyping data was analyzed with the FlowJo software by gating cell populations expressing the specific surface marker antigens (Fig. 1). The gating strategy from the initial flow cytometric data was initiated by first observing the total cell population using side scatter channel (SSC, y-axis) vs forward scatter channel (FSC, x-axis) plot. In flow cytometry, the amount of light scattered by the cells is measured at right angles to the laser beam (SSC) and forward direction (FSC). The size, morphology and optical homogeneity of the cells affect how much of the light is scattered. The fluorochromes in each tube were designed to delineate the different cell populations. After the gating process of different cell populations, the statistics were exported to FlowJo through Excel that were then converted to the CSV file format and linked with the Prism GraphPad Software to result in the final graphing of the data.

### Figure 1A | Gating of the cell populations using FlowJo

First, the SSC vs FSC plot was used to select the live cells out of the total cell population (excluding the granulocytes). The CD45<sup>+</sup> lymphocytes were gated next. From the CD45<sup>+</sup> population, the NK cells were gated as CD3-CD56<sup>+</sup>bright and CD3-CD56<sup>+</sup>dim cell populations. In addition, the total NK (dim and bright) were gated to see the total NK cell population. The CD3<sup>+</sup>CD56<sup>-</sup> T cells were gated in order to differentiate between the CD8<sup>-</sup> (CD4<sup>+</sup>) and CD8<sup>+</sup> T cells. Figure 1A shows the gating strategy for peripheral blood (healthy control).

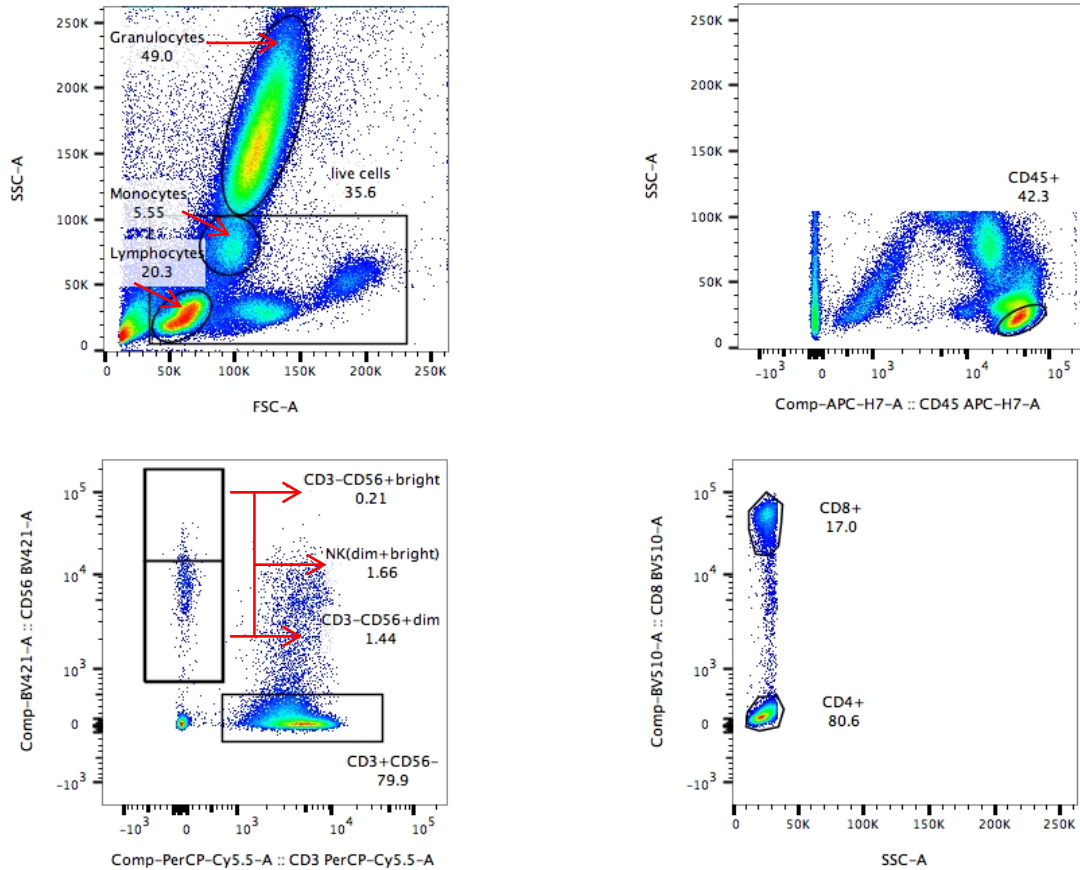


**Figure 1B | Gating of the RCC tumor samples**

The tumor samples were gated in a similar fashion as the peripheral blood. In addition, the CD4+CD8- and CD4-CD8+ populations were delineated in Tube B2 to avoid false positive and negative populations. The rest of the tubes from the antibody panel included the markers for CD3+ and CD8- that were then assumed as CD4+ T cells.

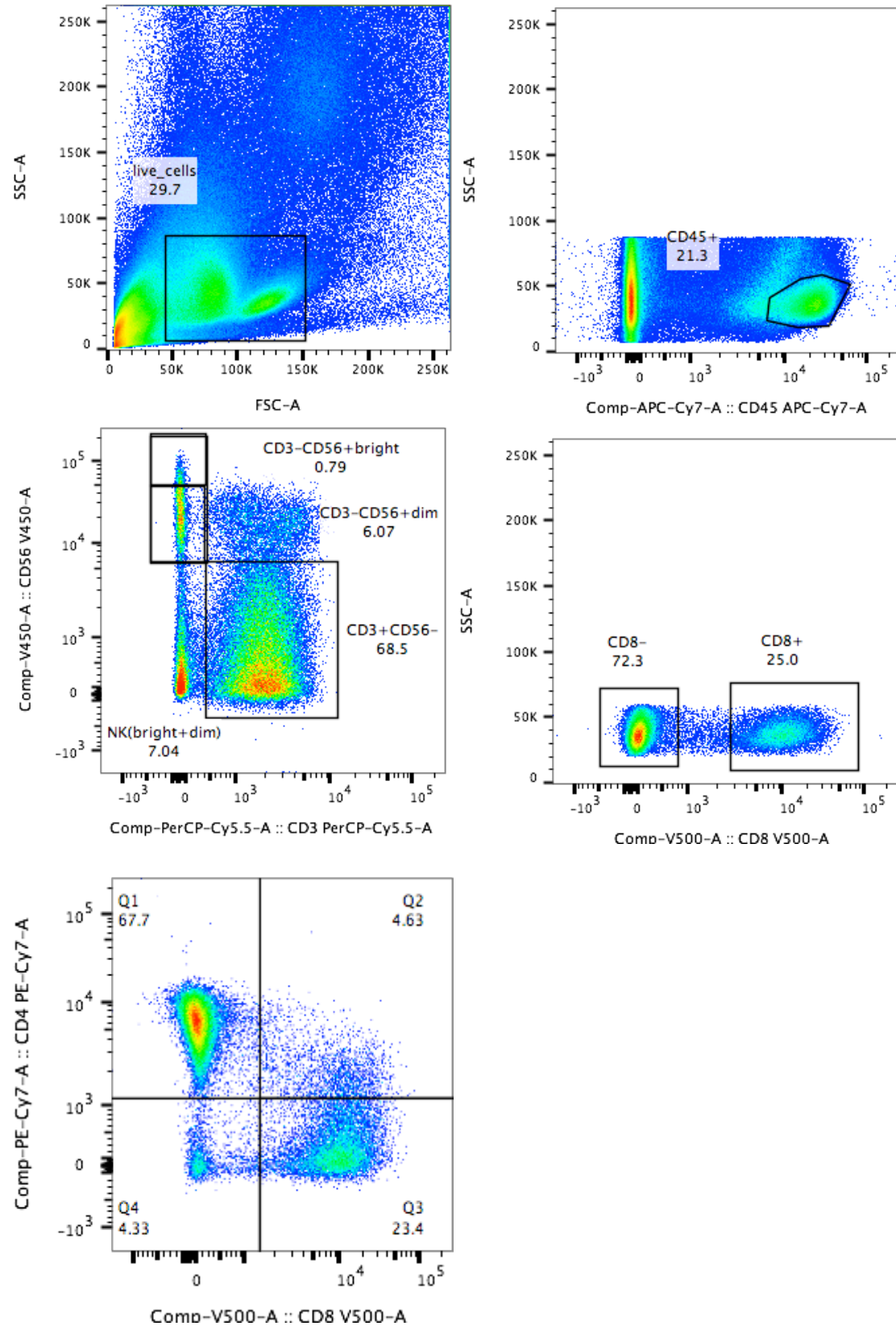
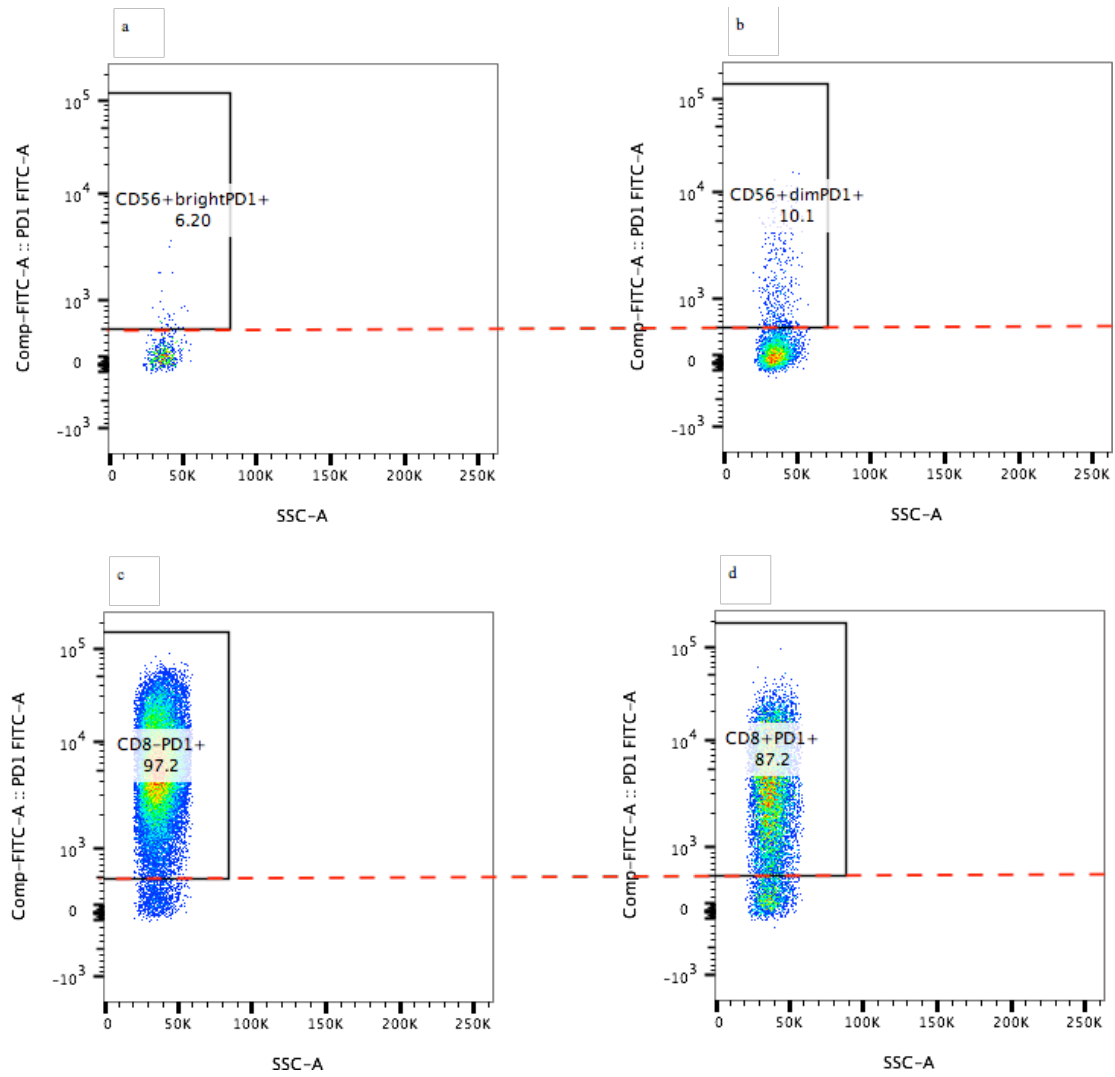




**Figure 1C | Expressions of specific receptors and surface markers were gated identically between different cell populations based on negative populations**

All the antibody markers in the CD4+ T, CD8+ T and CD56+ NK cells were gated in a consistent and identical fashion with reference to the negative cell populations. Here, the expression of PD-1 is demonstrated by gating the marker in the NK (CD3-CD56+ bright, dim), CD8- and CD8+ populations in a RCC patient sample.

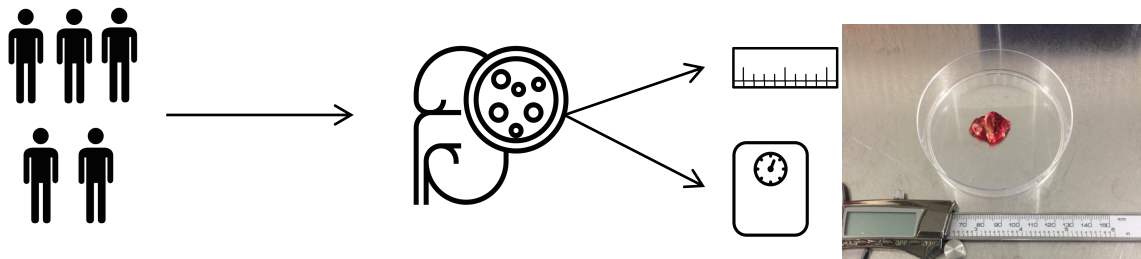


## Results

### RCC tumor characteristics

A total of 13 patient RCC tumor samples were received thus far and analyzed according to their size (diameter in mm) and weight (g) to distinguish the physical characteristics (Fig. 2.1). The median weight and diameter of the tumors were 3g (range 1.39-6.25g) and 22mm (range 15-33mm), accordingly (Fig. 2.2 a,b). The surgical nephrectomy procedure was kept consistent for all RCC patients, although exceptional cases are also present.

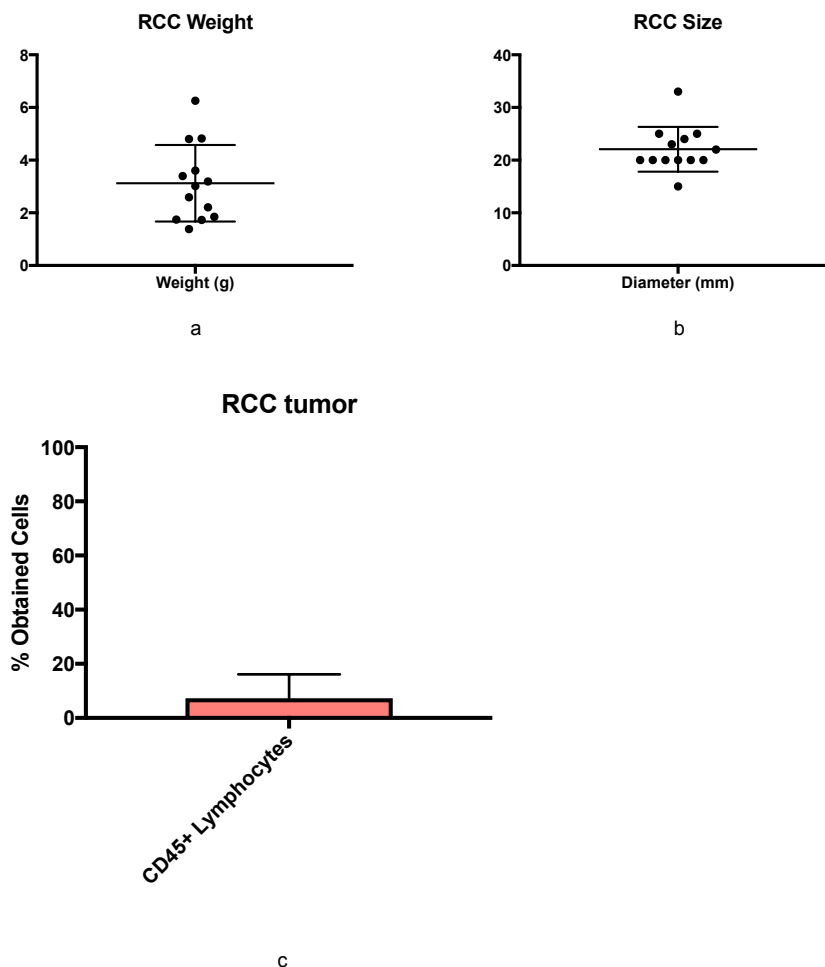
**Figure 2.1** | 13 RCC patient tumor samples have been collected thus far and were analyzed according to the tumor diameter and weight.



After the tumor was homogenized and dissociated (tumor dissociation kit, see materials and methods), a portion of the cells was immunophenotyped by flow cytometric analysis (approximately  $0.5 \times 10^6$  cells per tube). Then, the cells were further processed so that first, the lymphocyte population of cells could be gated. Next, the subpopulations of the lymphocytes (CD45+) in the population was isolated according to a distinct population that could be observed from the size of the CD45+ cell population in the SSC – CD45+ plot (see Fig 1b) according to the FlowJo gating strategy. The lymphocytes from the tumor were first gated from the live cell population that excluded the granulocytes and calculated from all total events; the CD45+ lymphocytes were then calculated from the lymphocyte live gate. 7.29% of the CD45+ lymphocyte population was obtained from the initial gating of the cells (Fig 2.2c).

### Figure 2.2 | RCC tumor characteristics

Each tumor before the immunophenotyping assay was weighed (g) and its diameter (mm) measured (a, b). During the flow cytometry analysis, the (c) The CD45+ lymphocyte population (mean = 7.29%) was gated from the initial cell population.



### The immunophenotype of TILs show an active phenotype in RCC patients

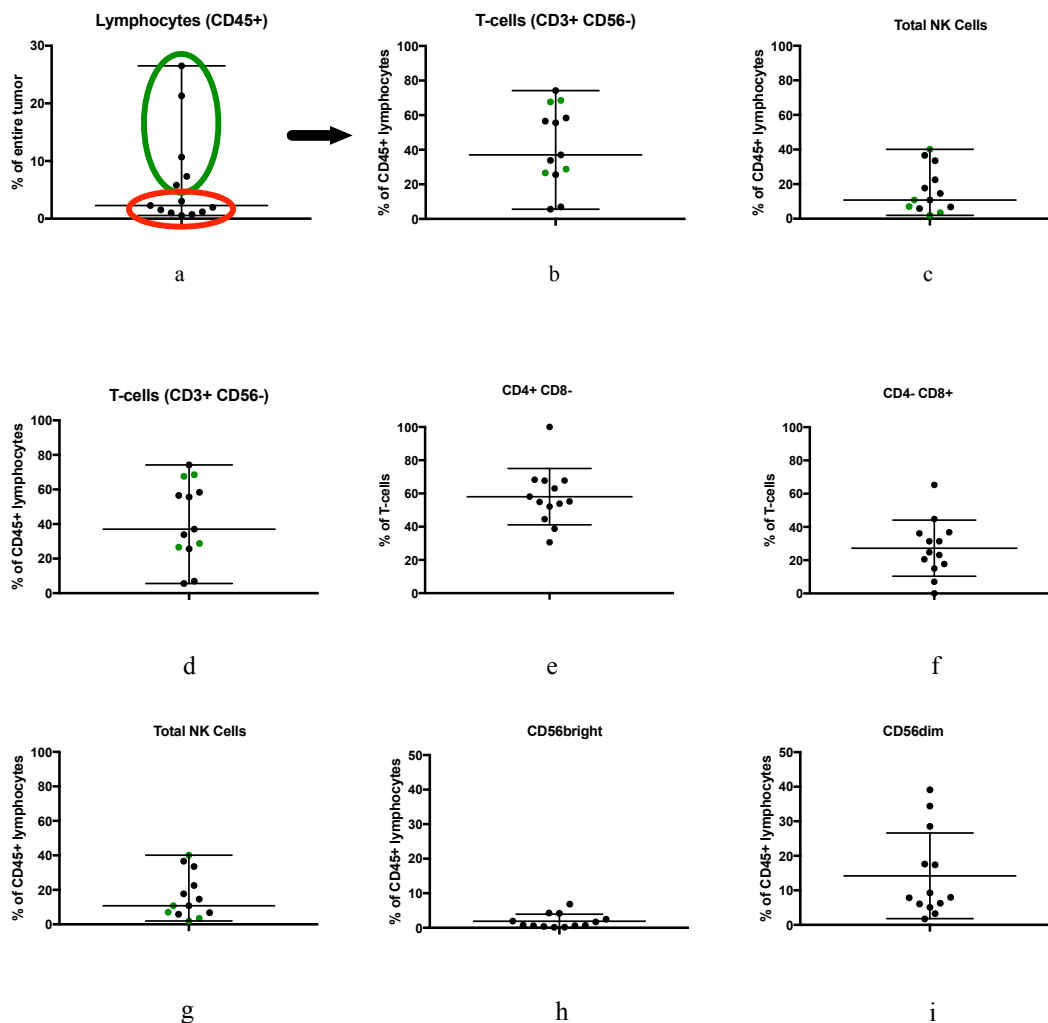
The patient-derived RCC samples were immunophenotyped by first homogenizing the tumor and staining the cells according to a specific antibody panel (Table 1) targeting NK, T cell and tumor-specific markers. The expressions were measured using flow cytometry. In order to gate and delineate the different cell populations expressing different surface antigens, the FlowJo software was used (Fig. 3). Out of the CD45+ lymphocytes, 37% were T cells and 10.8% NK cells on average (Fig. 3b, c). From the CD45+ lymphocyte population, the patients that had a high proportion of lymphocytes were grouped separately to see whether a similar pattern could be seen for the T and NK cells in the same patients. This was however not the case, as a high proportion of CD45+ lymphocytes did not indicate a large proportion of T and NK cells (Fig. 3a-c).

Consequently, we then analyzed the different TILs and their subset populations, namely the different CD4+, CD8+ T cells, and the CD56bright and CD56dim NK cells.

Amongst the T cell population, a higher percentage of CD4+CD8- cells were observed than the CD4-CD8+ cell population. Thus it can be concluded that there were more T helper and T memory (CD4+) cells in the RCC patient samples rather than the cytotoxic T cells (CD8+), indicating a higher CD4/CD8 ratio. From the total number of NK cells in the CD45+ lymphocytes, our results are concordant with the literature that states a higher amount of CD56 dim cells (Fig. 3i; mean = 14.19) are naturally present than CD56 bright NK subsets (Fig. 3h; mean = 1.91)<sup>14</sup>.

**Figure 3 | Immunophenotype of TILs in RCC patient tumor samples**

The homogenized tumor sample was stained with the antibody panel targeting the cells of interest (NK-, T-, and tumor-specific markers) and their expressions observed. (a) Green dots represent the patient samples that had the highest amount of the lymphocyte population from the flow cytometric analysis to see whether the amount of lymphocytes in the tumor was correlative to the amount of (b) T and (c) NK cell populations. (d) The T cells are divided into (e) CD4+CD8- and (f) CD4-CD8+ populations. (g) The NK cell population was divided into two subsets, (h) CD56bright and (i) CD56dim NK cell subpopulations gated from the CD45+ lymphocytes.



## Immune checkpoint markers are expressed in RCC TILs

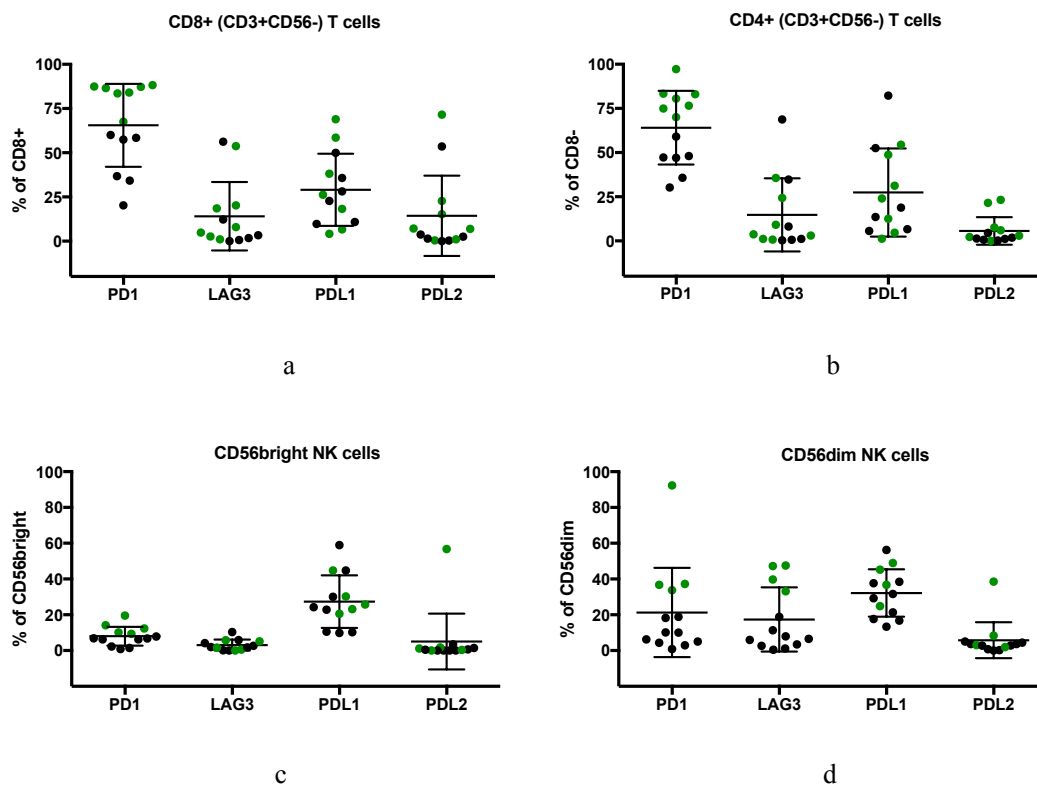
We investigated whether the patients with high expressions of PD-1 (green) also expressed high levels of other immune checkpoint markers, LAG-3, PD-L1 and PD-L2. Our results indicate that patients with a high expression in PD-1 do not express high levels of other immune checkpoint markers such as LAG-3 (Fig. 4a, b). The same can be said for the NK subset populations. Of particular note are the low expression levels of PD-1 and LAG-3 in the CD56bright as opposed to the higher expressions in the CD56dim NK subset (Fig. 4c, d).

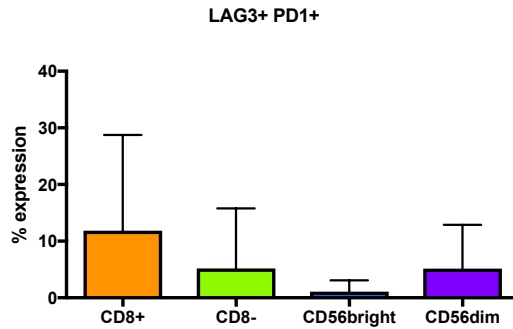
## PD-1/LAG-3 double positive expression

We were also interested in observing the PD-1/LAG-3 double positive expressions in the TILs (Fig 4e). PD1 was highly expressed in both CD8+ and CD4+ T cells, but the highest amount of double positive cells was seen amongst the CD8+ T cell population (approximately 10% of the CD8+ T cells), known as the main effector of anti-tumor responses<sup>15</sup>.

## Figure 4 | Expression of immune checkpoint markers in TILs

In this figure, the expression profiles of the RCC immune cells involving the mAbs PD-1, LAG-3, and the PD-L family of markers are shown for (a) CD8+ T cells, (b) CD4+ T cells, (c) CD56bright NK cells, and (d) CD56dim NK cells. Figure (e) shows the LAG-3/PD-1 double positive expression in T (CD8+, CD8-) and NK (CD56bright, CD56 dim) cell subsets. The double positive expression occurs the highest in the CD8+ T cell population.





e

### CXC chemokine receptor expression in RCC tumors

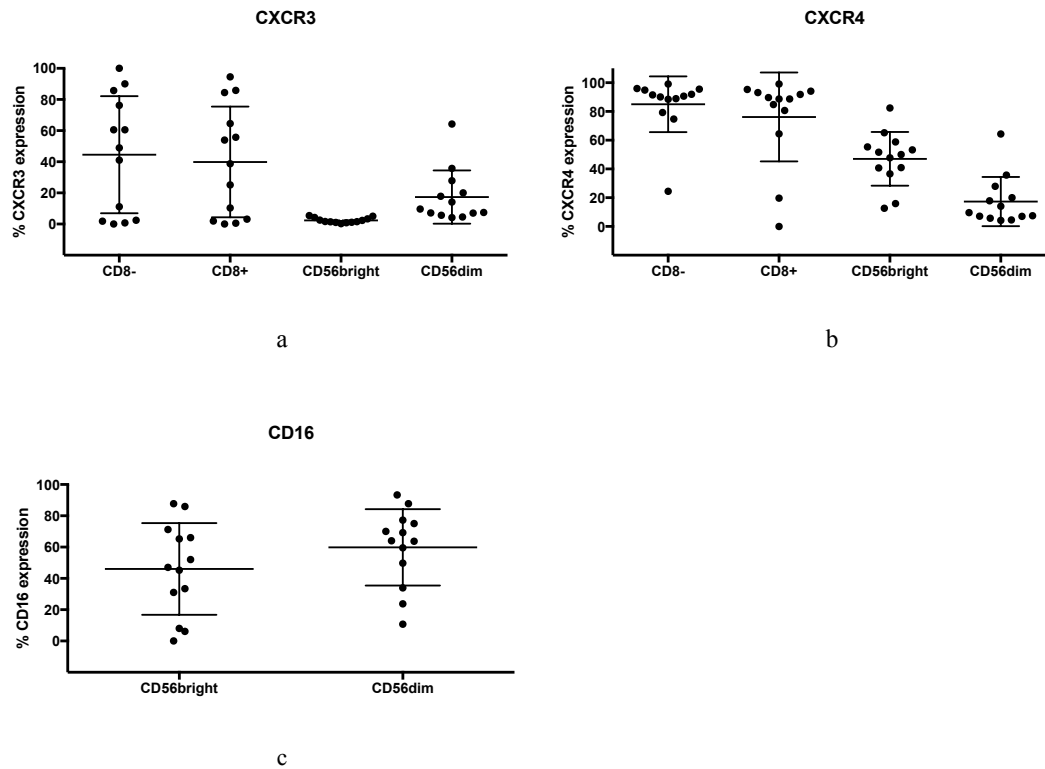
To further characterize the intratumoral lymphocytes, we analyzed the CXC chemokine receptor expressions (CXCR3 and CXCR4) in the RCC tumors (Fig. 5). The CXCR3 expression varied amongst the patients. Of particular note, the CD56bright NK cells hardly expressed the CXCR3 receptor, whereas the CD56dim cells showed a higher amount of expression (Fig 5a). Also, a higher proportion of the patients expressed CXCR4 as opposed to CXCR3 in both T and NK cells (Fig 5b). Although CXCR3 expression is highly variable in the T cells, the expression of CXCR4 follows an increased and similar pattern of expression amongst the RCC tumors.

### CD16 is highly expressed in NK cells

Next, we looked at the CD16 expression in both subsets of the NK cells (Fig 5c). CD16 is a low affinity receptor (FcγRIII) that binds to the constant Fc chain of the antibody, activates the NK cells, and induces antibody-dependent cellular cytotoxicity (ADCC), resulting in lysis of the target cell<sup>16,17</sup>. Our results indicate that CD16 is thus expressed in both NK subsets and more in the CD56dim subpopulation.

### Figure 5 | Expression profiling of the RCC tumor cells involving the CXC chemokine receptors and CD16 markers

**(a)** The percentage CXCR3 expression given for T (CD8-, CD8+) and NK (CD56bright, CD56dim) cells. Our results indicate a higher expression of CXCR3 in T cells when compared to the expression in the NK cell subsets. **(b)** CXCR4 expression is also higher in T cells when compared to NK cells, with similar patterns of expression in the T cell populations. **(c)** CD16 is highly expressed in both NK subsets.



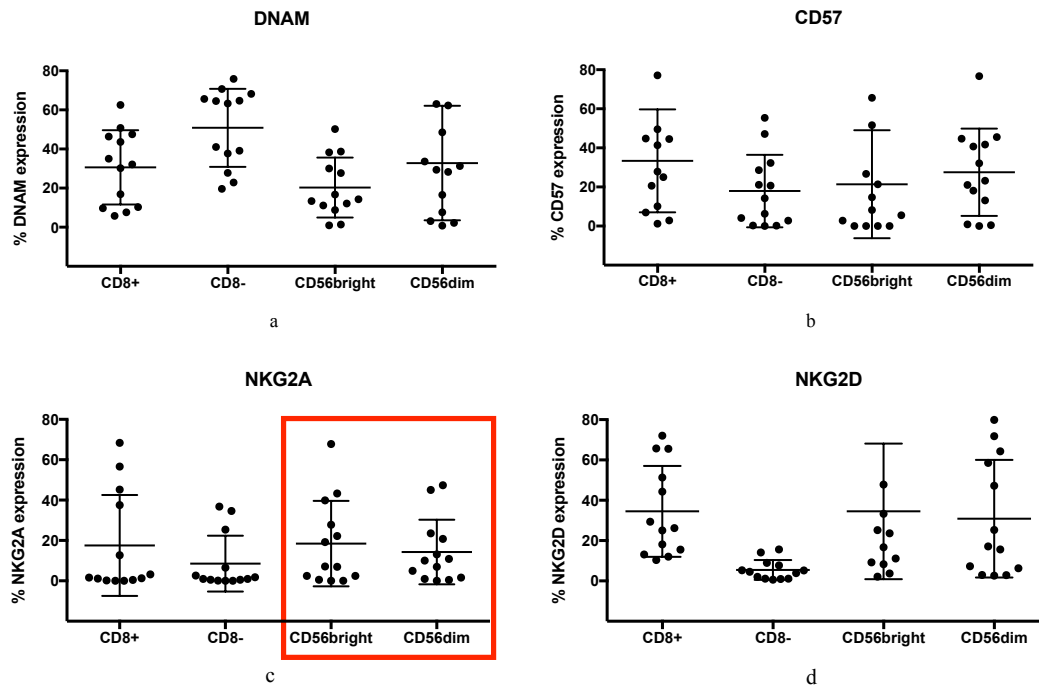
### Markers of NK cell activation

Although markers such as DNAM and CD57 showed variable expressions on the T and NK cells, their patterns of distribution can further be divided into subpopulations amongst the patients. An elevated expression of DNAM could be observed when compared to CD57 (Fig. 6a, b), indicative of activation in the natural cytotoxicity receptor. CD57 is a marker for highly differentiated NK cells<sup>18</sup>. The expression pattern was observed to be similar between the CD8- T cells and CD56bright NK population.

Next, we looked at the NKG2 family of receptors involved in NK cell receptor activation. The NK cell populations showed a high expression of the NKG2A marker (Fig. 6c). With respect to NKG2D expression, only a small subset of cells expressed the marker in the CD4+CD8- T cells (Fig. 6d), which is agreeable with the literature showing that only a small population of CD4+ T cells naturally express NKG2D<sup>19</sup>. The CD8+ T cells and the CD56dim NK cells also showed distinct subgroups of the patients that expressed high and low levels of the NKG2D marker.

### Figure 6 | Expression profiling of the RCC tumor cells involving the NKG2 family, DNAM and CD57 markers

(a) DNAM expression in the different lymphocyte subpopulations. The highest expression could be seen for the CD8- T and CD56dim NK cells. (b) CD57 expression varied between patients. (c) Higher NKG2A expression in NK cell subsets than in T cells. Many RCC tumors indicate a similar pattern of expression in T cells. (d) Low NKG2D expression in CD8- T cells was observed compared to CD8+ T cells.



### Tumor specific markers and their immune profiles

In our uniquely designed antibody panel (Table 1), the final tube (B4) consisted of the markers that were selectively included to target the tumor cells from the rest of the cells in the sample. Also, the gating of the cells was done in a similar fashion as above so that the lymphocytes and tumor cells could be differentiated. It should be noted that the RCC tumors were transported to our facilities for processing as soon as the circulation of the nephrectomy was cut off to ensure maximal cell viability. Our results show that the majority of the cells obtained were viable based on the viability marker, 7-AAD (mean = 87.63%; Fig. 7b). The viable cells were then divided to CD45+ leukocytes and CD45- cell populations, which presumably consisted mostly of the tumor cells (Fig. c, d). The majority of cells were CD45-, thus being mostly tumor and stromal cells (mean = 90.8%; Fig. 7d).

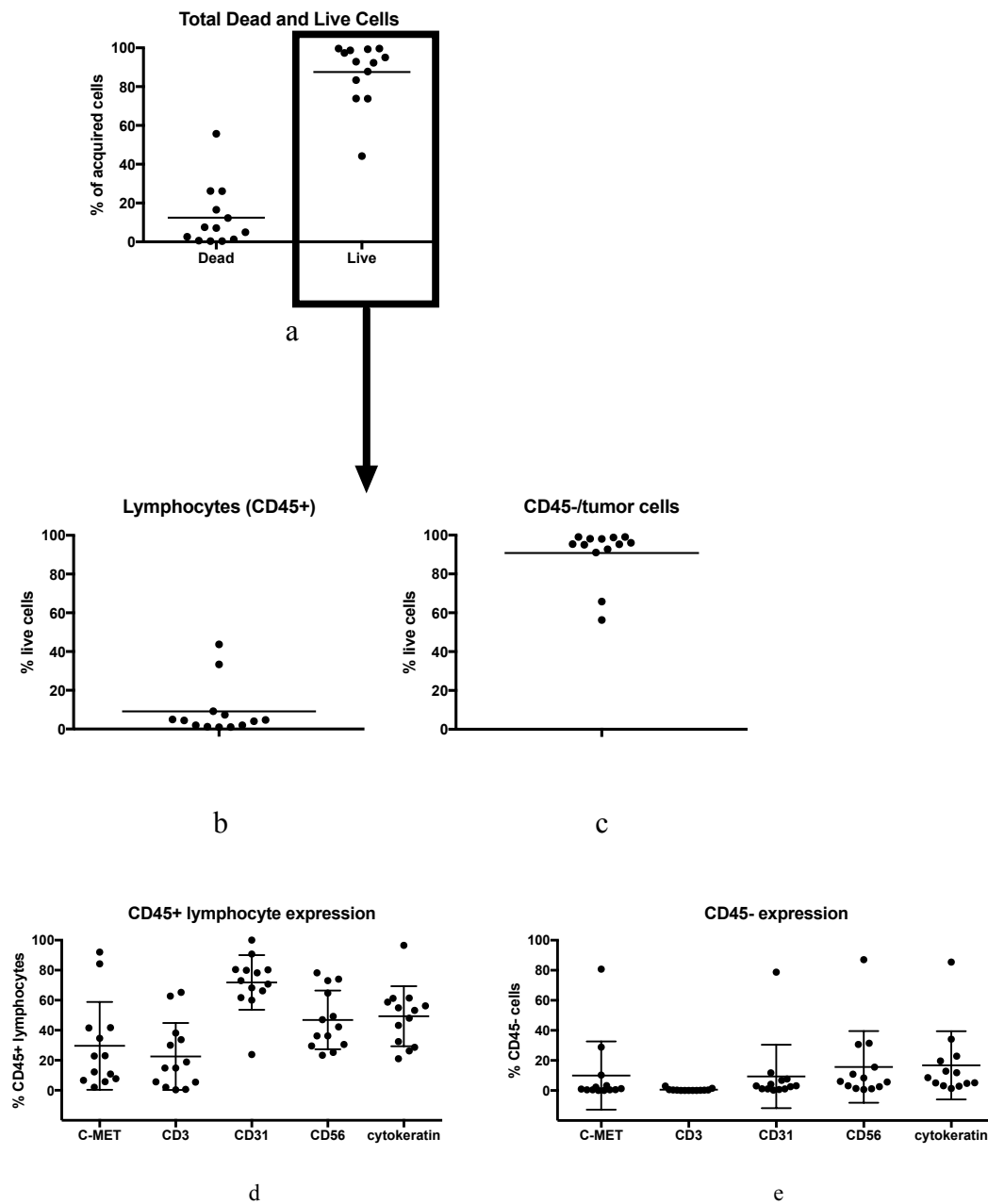
Next, we wanted to test the lymphocytic and tumor cell subpopulations with tumor-specific markers in order to observe their immunophenotypes. To our surprise, the cytokeratin and C-Met staining was also observed in CD45+ lymphocytes (Fig. 7e, f). Although C-Met is considered to be critical in playing a role in the growth of RCC by increasing PD-L1 expression and anti-apoptotic signals<sup>20</sup>, the expression of the marker was low in most of the



tumor cells. In addition, most of the tumor cells expressed low amounts of cytokeratin, a marker associated with the differential diagnosis of renal tumors<sup>20</sup> (Fig. 7f). Further analyses are needed to clarify the specificities of the antibodies.

**Figure 7 | Tumor-specific markers and their expression profiles from the RCC tumor cells**

(a) From the total cells, we gated the negative and positive cell populations (dead and live, respectively) using the FlowJo software. (b) The CD45+ lymphocytes and (c) CD45- population that contains the tumor and stromal cells. (e) Expression of tumor cell markers on the CD45+ lymphocytes and (f) on the CD45- cells that were presumed to contain tumor cells.



### **RCC cell lines are able to grow into 3D spheroids *in vitro***

In order to create an *in vitro* experiment where we could grow tumor 3D models, spheroids using RCC cell lines were cultured and their morphologies observed. After the fourth day of seeding, the single-cell suspensions of the RCC cell lines A-498 and CAKI-1 were able to grow in each well, whereby a spherical structure could be observed under a phase-contrast microscope. Consequently, the spheroids maintained their form and structure for the remainder of the days in which their growths were followed. Owing to the different cell lines, the A-498 cells were smaller in size (mean = 300 $\mu$ m) and maintained a circular structure (Fig. 8A). The CAKI-1 cells on the other hand, grew to a more spherical, blooming structure (Fig. 8B), and were larger in diameter (mean = 700 $\mu$ m).

After a 30-day analysis of the cells, many of the cellular suspensions became contaminated and were not viable. Under the microscope, it could be observed that the cells became necrotic or could no longer be visualized, due to the contaminated environment of the plate wells. Out of the 96 wells of the plate, half of the plates were seeded with A-498 and the other half with CAKI-1 cells. After a 30-day observation, less than 50% of the seeded cells discontinued their growth or survived. However, the remaining cells were still able to retain their size and morphology. Our results confirmed the 3D spheroids could be grown *in vitro* from RCC cell lines.

#### **Figure 8 | 3D tumor spheroid model, A-498 and CAKI-1**

The RCC cell lines A-498 and CAKI-1 were plated as single cell suspensions per well. Their size and morphology were followed after seeding. As a result, the cells were able to form spheroids from approximately the fifth day of plating the cells. The size and morphology of the cells remained consistent during and after their growth for 30 days (from left to right: d3, d5, d7...d30).

#### **Figure 8A | 3D tumor spheroid model, A-498**

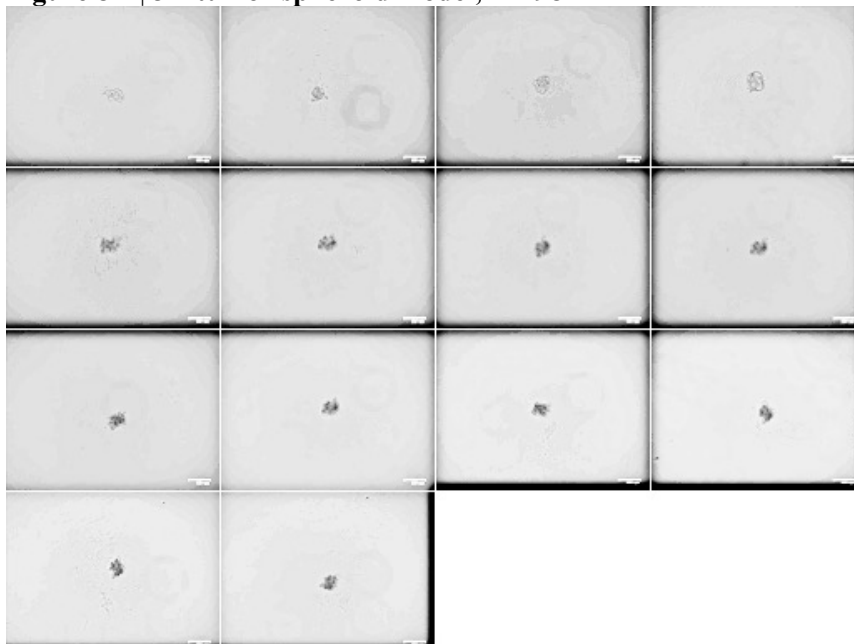
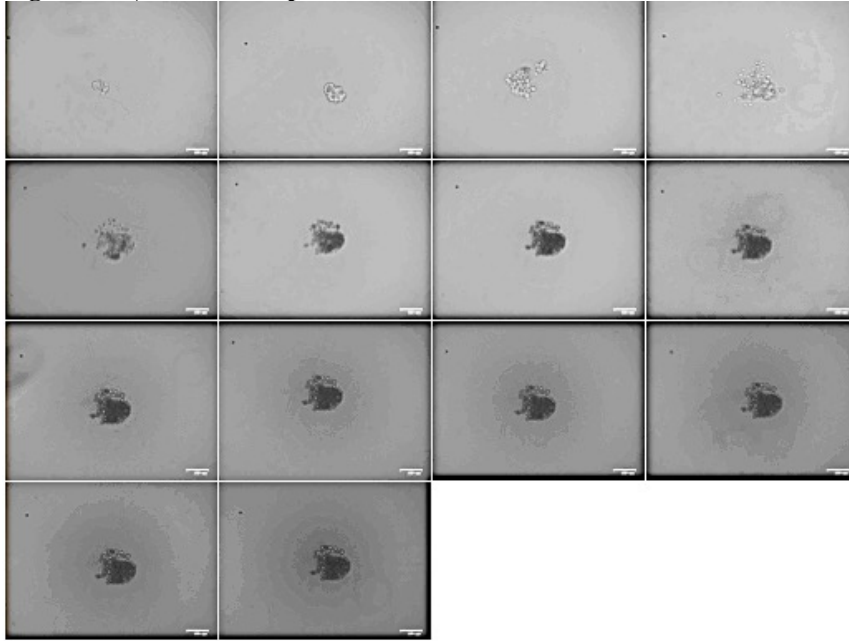


**Figure 8B | 3D tumor spheroid model, CAKI-1**



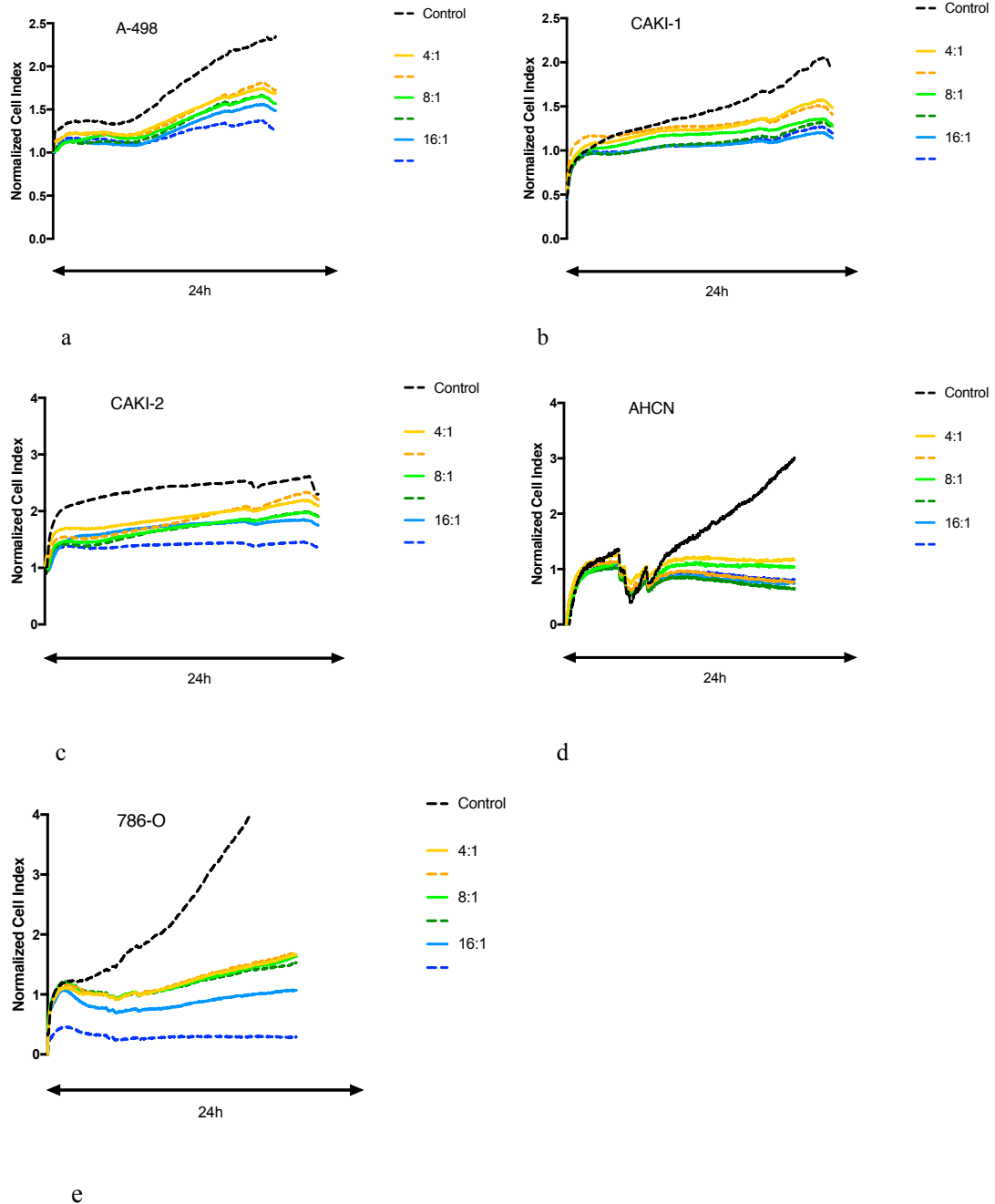
**RCC cell lines are sensitive to NK cell-mediated cytotoxicity**

The target RCC cell lines A-498, CAKI-1, CAKI-2, AHCN and 786-O were tested by co-incubating them with the cytotoxic NK-92 cell line to see whether they were suitable for NK cell-mediated killing. The cell lines were initially plated in duplicate ratios using the iCelligence 8-well plates and were incubated overnight so that a monolayer of the cells could form. After a 24h incubation period, the effector NK-92 cell lines were plated together with the target cells and incubated for another 24h in order to fully observe their cytotoxic effects.

The results indicate that the NK-92 cells were able to effectively kill each target cell line. Furthermore, this cytotoxic activity is increased with higher E:T ratios (Fig. 9). The cytotoxic events may be observed by comparing the control well, whereby only the target cells were plated. Here, the cellular impedance (CI) steadily increases over time, indicating cellular proliferation and confluence. Similar curves were observed for the cytotoxic activity in the cell lines. As the E:T ratios increased (4:1, 8:1, 16:1), the cytotoxic effects of the NK-92 cells increased, in which the greatest cytotoxicity could be observed with the highest E:T ratio. The cytotoxic function of the effector cells with the 4:1 and 8:1 ratios did not have a vast difference towards the target cells, although it could be clearly seen that the increased E:T ratio resulted in more cytotoxic behavior. Out of the various RCC cell lines that were tested, the 786-O cells showed the most vigorous cytotoxic effect (Fig. 9e). From our observations, the target and effector cell lines were confirmed to be suitable for the direct cytotoxic assay.

### Figure 9 | Cytotoxic activity of the NK-92 (effector) cell line towards the RCC (target) cell lines

The effector and target cell lines were co-incubated for 24h in which the CI was measured every minute. Each E:T ratio was plated as duplicates (line and dotted lines). The normalized CI increases in the control well, indicating target cell growth. The CI decreases in the E:T wells according to the increasing E:T ratios, indicating an increase in cytotoxic activity.



## Discussion

Our adaptive and innate immune systems have shown the potential to clear cancer. Targeting immune checkpoints, and thus activating the immune system to kill cancer, have become a promising treatment option for cancer immunotherapy in a variety of different cancers, starting from metastatic melanoma and further, to RCC among others. This type of therapy aims to show good clinical response as well as benefit the overall patient survival rate. Despite this hope, the immune checkpoint proteins that we know so far such as PD-1 only make up a tiny piece of the puzzle out of a plethora of ligands and receptors that may be potential immunotherapy targets. Immune checkpoint pathways that are dominant in the tumor microenvironment are key players in the identification of potential immunological biomarkers. In order for their detection, it would be crucial to determine which pathways are commanding the particular tumor. Likewise, other challenges remain, such as the need to improve the combinatorial effects of the therapy in the clinical environment. Monotherapies such as anti-PD-1 are deemed more efficacious when combined with other forms of targeted therapies such as the use of vaccines that will provide further antitumor immunity<sup>7</sup>. In addition, NK cells have the ability to potentiate strong antitumor activity, but their importance and influence are yet to be explored further.

### **The unique tumor immunophenotype of each RCC patient**

The regulation of T cell function is known to be involved in an array of mechanisms including the activation of coinhibitory molecules that suppress the signaling pathways. One such set of signals is mediated by programmed death protein 1 (PD-1) and programmed death ligand 1 (PD-L1) that are part of the CD28/CTLA-4 (cytotoxic T-lymphocyte-associated protein 4) family and are activated in T cells. Upon binding with its ligands, PD-L1 and PD-L2 become negative regulators of T cell receptor (TCR) signaling, decreasing T cell proliferation and cytokine production<sup>3</sup>.

PD-1 is thus responsible for the downregulation of the immune system and promotes self-tolerance by suppressing T cell-induced inflammatory activity. From our results, we observed that the high expression of PD-1 does not correspond to similar expression levels for other immune checkpoint molecules such as LAG-3 (Fig. 4). In addition, the low PD-1 expression observed in the CD56<sup>bright</sup> NK cells did not signify similar expression levels for the CD56<sup>dim</sup> NK subsets (Fig. 4c, d). In-depth functional studies targeting the different NK cell subsets and their significance in expressing different levels the immune checkpoint markers are further needed. We also explored the PD-1 and LAG-3 double positive

expressions in the TILs, and noticed that the highest expression occurs in CD8+ T cells (Fig. 4e). Further analyses are needed to investigate whether the combination of the proteins may serve as a possible prognostic marker for RCC similarly, as is the case in patients diagnosed with triple negative breast cancer and express both checkpoint receptors<sup>15</sup>.

The CXC chemokine receptors CXCR3 and CXCR4 are markers that are mainly expressed in B, T and NK cells and are responsible in regulating the migration of cells. Here, we were particularly interested in the migration of T and NK cells. A high expression of CXCR4 could be seen in most of the patient tumors (Fig. 5). This may be due to the fact that CXCR4 is a functional receptor that is upregulated in cancerous cells compared to healthy tissue<sup>21</sup>. It has also previously been shown that CXCR4 expression is correlated with the metastatic potential of RCCs, and is overexpressed in primary tumors<sup>22</sup>. The high expression may thus be correlative to an increased tendency of the RCC tumors to metastasize outside the kidney. CD16 is considered to have constitutive expression in CD56dim NK cells that may in turn result in an increased number of Fc $\gamma$ RIII-bearing NK cells and enhance their activation<sup>16</sup>. For solid tumors, the loss of CD16 in tumor infiltrating NK cells is associated with the loss of NK cell-tumor engagement, diminished tumor recognition and cytotoxicity ADCC<sup>16,17</sup>. In our study, we observed that CD16 was expressed in both NK cell subsets (Fig. 5c).

The NKG2 family of proteins is mostly expressed on the surface of naïve NK cells and is responsible for the activation of NK cells<sup>19</sup>. In healthy cells, the receptors are tightly regulated in order to prevent autoimmune and self-recognition reactivity. We observed a heightened expression pattern in the NK cells of the RCC patient tumors for the NKG2A receptor compared to the T cells (Fig. 6c). A follow-up study comparing the circulating NK cells in the blood from the same patients before (tumor) and after (peripheral blood) their surgery would be one method to see a difference in the expressions of the marker. Also, NKG2D is expressed in all CD8+ T cells, on most NK cells, and only in a subset of CD4+ T cells<sup>25</sup>. Our results are in accordance with this indicating a low expression of NKG2D in the CD4+ T cells and high expression of the marker in all CD8+ T cells of the RCC patient tumors (Fig. 6d). We also observed a subgroup of patients whose CD8+ T cells and CD56dim NK cells had particularly high expression of NKG2D, which may be an indication of inflammation<sup>19,25</sup>.

With regards to targeting the lymphocytic and tumor cell subpopulations, we added the c-Met marker into our antibody panel. C-Met is known as tyrosine-protein kinase Met, whereby mutations in the MET gene are commonly associated with papillary RCCs. Also, c-Met serves as a prognostic marker and potential therapeutic target in RCC<sup>26</sup>. Together with cytokeratin, these two antibodies were considered as markers for tumor cells, as we wanted to observe how many tumor cells were in each sample. However, it seemed that the antibodies

also bound to lymphocytes and therefore, the panel needs further optimization of the tumor-specific markers that will directly and specifically target the tumor cells. One solution would be to add more immunomarkers that concern kidney tumors, such as cytokeratin 18 (CK18) which is positively expressed in all major types of renal tumors, and ‘RCC marker (the commercial name by Vector Laboratories Inc),’ a mAb directed against a glycoprotein found in the brush border of healthy renal proximal tubular cells<sup>27</sup>.

So far, targeting the PD-1 and PD-L1 blockade has shown the most promise in the treatment of solid tumors, including RCC with noticeable antitumor effects, increased treatment responses and overall survival rates of the patients<sup>28</sup>. In melanoma patients, anti-PD-1 acts as lymphocyte activators, in which the inhibitory signals to the checkpoint inhibitor, PD-1 are blocked. This effect enables the cytotoxic T cells to regain their cytotoxic capabilities against the cancer. Because anti-PD-1 is known to restore antitumor T cell functioning in melanoma, this effect may also be observed in renal cancers. However, one aspect of research would be to further investigate how anti-PD-1 treatment affects the NK cells and their cytotoxic ability. Although the enhancing effects of anti-PD-1 to NK cell mediated cytotoxic activity has been reported for *in vitro* studies using NK cells derived from myeloma patients<sup>29</sup>, further research is needed in exploring the effects on the immunophenotype of NK cells, as well as on the functional activities the cells have *in vivo* for patients treated with anti-PD-1.

Our results showed that RCC patients have variable immune checkpoint expressions in their TILs. One example is the variability in PD-1 expression, as some patients had high expressions of the marker, whereas others had low expression. Another interesting phenotype was the PD-1 and LAG-3 double positive cells. Further research is needed to assess the patients who express high levels of both markers, providing potential candidates for combinatorial therapies and better predictors of patient screening for future clinical trials. The highly unique aspects of the immune profiles as well as the shared tumor characteristics shed more insight on the future of immuno-oncological therapies and possibly, new breakthroughs for biomarker studies.

### **NK cells possess cytotoxic activity against RCC**

To measure the cytotoxic potential of the NK-92 cell line against the RCC cell lines, the real time killing assay was used. This method could be further applied in testing the RCC patients’ NK cells towards the target cell lines. Our results are in accordance with the literature that has shown that NK cells are able to target and kill cancer cells without pre-stimulation<sup>13</sup>. The differences observed in the killing activities of the NK-92 effector cells against the different target cell lines may be due to the variability in morphology, growth and doubling time. This is due to the instrument’s impedance-based characteristics in measuring the different types of

adherent cells that have attached to the bottom of the wells. Also, the interactions between the target and effector cells might unleash different molecular interactions that may inhibit or slow down the killing process. Another factor that could be accountable for the different readouts may be due to the variable immunogenic characteristics between the cell lines, and this should be further studied (such as the expression of various ligands that activate and/or inhibit NK cell receptors).

Follow up studies involving the cytotoxic potentials of *in vivo* patient NK cells are much needed. One aspect to keep in mind would be the tumor microenvironment, and how it can affect the tumor cells as well as the tumor infiltrating immune cells. Other factors include epigenetic and environmental factors, such as age and smoking. Renal cancers are very much age-related, whereby the stage of onset and diagnosis occurs later in life and among the elderly. Furthermore, it should be noted that the immune system varies greatly with age (such as the reduced diversity of T cells in the elderly<sup>30</sup>), providing further evidence for the loss of immune cell control in older people. It has also been observed that smokers are liable to having low NK and immunoglobulin numbers, which may affect their overall immune systems and ability to fight off certain diseases<sup>31</sup>. With this in mind, the number of patients in our study is currently too small to compare the effect of age on the different immune cells.

We also noticed that there is considerable inter-individual variation among the RCC patients. However, the depth of the variation is still yet unclear and needs detailed analyses using multiplexed systems such as mass cytometry. By considering these inter-dependent components of the immune system, we may be able to further explore the co-variation between health and disease<sup>31</sup>. Recent cohort studies have already shown great variability in the immune cell frequencies in healthy adults, such as the frequency of CD4<sup>+</sup> T cells ranging between 22 – 90%; CD8<sup>+</sup> T cells between 6 – 65%; and NK cells, 0 – 59%<sup>32,33</sup>. The observation that healthy individuals possess such a wide degree of variation in immune cells suggests novel studies for the future.

### **3D *ex vivo* tumor models**

The preliminary data from the *in vitro* spheroid models suggest that the growth and monitoring of the RCC cell lines are possible. However, the model still lacks various optimization steps until various immune checkpoint inhibitors and TIL-associated markers can be tested. We are currently exploring another 3D tumor model using patient-derived RCC cells, which would greatly improve our research aims in testing the functional characteristics, as well as to analyze cell-to-cell contacts for future assays.



### **Patient pre-surgery and follow-up samples**

To characterize further the TILs and RCC tumor cells, we hope to receive peripheral blood samples in addition to the tumor tissue both pre- and post-surgery. Analyses between the immunophenotypic expressions before the surgery as well as after the patient's recovery would be vital in comparing them with the results that we have managed to get from the tumor immune profiles thus far.

In conclusion, we have characterized the immune phenotypes of the patient-derived RCC tumor cells and TILs with various immune checkpoint markers. Based on our preliminary phenotypic data and cytotoxicity assays, we state that NK cells have the potential to become actively cytolytic, and potentially enhance the antitumor immunity by acting on the RCC cells *in vitro*. Our results also indicate that there are unique inter-individual differences between the patients. Further analyses and a larger number of patients are necessary components to compare the differences and shared characteristics between the tumor and blood samples. In the future, we hope to broaden our knowledge in comparing and distinguishing the fundamental roles of the two cytotoxic lymphocytes, the NK and T cells, as well as their roles in the clearance of cancer under the influence of immune checkpoint inhibitors.

## References

1. Siegel, R. L., Miller, K. D., & Jemal, A. (2017). Cancer statistics, 2017. *CA: A Cancer Journal for Clinicians*, 67(1), 7-30. doi:10.3322/caac.21387 [doi]
2. The NORDCAN project, Association of the Nordic Cancer Registries <http://www-dep.iarc.fr/NORDCAN/english/frame.asp>
3. Carlo, M. I., Voss, M. H., & Motzer, R. J. (2016). Checkpoint inhibitors and other novel immunotherapies for advanced renal cell carcinoma. *Nature Reviews.Urology*, 13(7), 420-431. doi:10.1038/nrurol.2016.103 [doi]
4. Iwai, Y., Ishida, M., Tanaka, Y., Okazaki, T., Honjo, T., & Minato, N. (2002). Involvement of PD-L1 on tumor cells in the escape from host immune system and tumor immunotherapy by PD-L1 blockade. *Proceedings of the National Academy of Sciences of the United States of America*, 99(19), 12293-12297. doi:10.1073/pnas.192461099 [doi]
5. Atkins, M. B., Clark, J. I., & Quinn, D. I. (2017). Immune checkpoint inhibitors in advanced renal cell carcinoma: Experience to date and future directions. *Annals of Oncology : Official Journal of the European Society for Medical Oncology*, doi:10.1093/annonc/mdx151 [doi]
6. Quinn, D. I., & Lara, P. N., Jr. (2015). Renal-cell cancer--targeting an immune checkpoint or multiple kinases. *The New England Journal of Medicine*, 373(19), 1872-1874. doi:10.1056/NEJMe1511252 [doi]
7. Pardoll, D. M. (2012). The blockade of immune checkpoints in cancer immunotherapy. *Nature Reviews.Cancer*, 12(4), 252-264. doi:10.1038/nrc3239 [doi]
8. Zamai, L., Ponti, C., Mirandola, P., Gobbi, G., Papa, S., Galeotti, L., et al. (2007). NK cells and cancer. *Journal of Immunology (Baltimore, Md.: 1950)*, 178(7), 4011-4016. doi:178/7/4011 [pii]

9. Ansell, S. M., & Vonderheide, R. H. (2013). Cellular composition of the tumor microenvironment. American Society of Clinical Oncology Educational Book. American Society of Clinical Oncology Meeting, doi:10.1200/EdBook\_AM.2013.33.e91 [doi]
10. Vey, N., Bourhis, J. H., Boissel, N., Bordessoule, D., Prebet, T., Charbonnier, A., et al. (2012). A phase 1 trial of the anti-inhibitory KIR mAb IPH2101 for AML in complete remission. *Blood*, 120(22), 4317-4323. doi:10.1182/blood-2012-06-437558 [doi]
11. Gong, J. H., Maki, G., & Klingemann, H. G. (1994). Characterization of a human cell line (NK-92) with phenotypical and functional characteristics of activated natural killer cells. *Leukemia*, 8(4), 652-658.
12. <http://www.aceabio.com/wp-content/uploads/Label-Free-Assay-for-NK-Cell-Mediated-Cytolysis.pdf>
13. Zhu, J., Wang, X., Xu, X., & Abassi, Y. A. (2006). Dynamic and label-free monitoring of natural killer cell cytotoxic activity using electronic cell sensor arrays. *Journal of Immunological Methods*, 309(1-2), 25-33. doi:S0022-1759(05)00409-6 [pii]
14. Cooper, M. A., Fehniger, T. A., & Caligiuri, M. A. (2001). The biology of human natural killer-cell subsets. *Trends in Immunology*, 22(11), 633-640. doi:S1471-4906(01)02060-9 [pii]
15. Bottai, G., Raschioni, C., Losurdo, A., Di Tommaso, L., Tinterri, C., Torrisi, R., et al. (2016). An immune stratification reveals a subset of PD-1/LAG-3 double-positive triple-negative breast cancers. *Breast Cancer Research : BCR*, 18(1), 121. doi:10.1186/s13058-016-0783-4 [doi]
16. Poli, A., Michel, T., Theresine, M., Andres, E., Hentges, F., & Zimmer, J. (2009). CD56bright natural killer (NK) cells: An important NK cell subset. *Immunology*, 126(4), 458-465. doi:10.1111/j.1365-2567.2008.03027.x [doi]

17. Gras Navarro, A., Bjorklund, A. T., & Chekenya, M. (2015). Therapeutic potential and challenges of natural killer cells in treatment of solid tumors. *Frontiers in Immunology*, 6, 202. doi:10.3389/fimmu.2015.00202 [doi]
18. Kared, H., Martelli, S., Ng, T. P., Pender, S. L., & Larbi, A. (2016). CD57 in human natural killer cells and T-lymphocytes. *Cancer Immunology, Immunotherapy* : CII, 65(4), 441-452. doi:10.1007/s00262-016-1803-z [doi]
19. Raulet, D. H. (2003). Roles of the NKG2D immunoreceptor and its ligands. *Nature Reviews.Immunology*, 3(10), 781-790. doi:10.1038/nri1199 [doi]
20. Balan, M., Mier y Teran, E., Waaga-Gasser, A. M., Gasser, M., Choueiri, T. K., Freeman, G., et al. (2015). Novel roles of c-met in the survival of renal cancer cells through the regulation of HO-1 and PD-L1 expression. *The Journal of Biological Chemistry*, 290(13), 8110-8120. doi:10.1074/jbc.M114.612689 [doi]
21. Skinnider, B. F., Folpe, A. L., Hennigar, R. A., Lim, S. D., Cohen, C., Tamboli, P., et al. (2005). Distribution of cytokeratins and vimentin in adult renal neoplasms and normal renal tissue: Potential utility of a cytokeratin antibody panel in the differential diagnosis of renal tumors. *The American Journal of Surgical Pathology*, 29(6), 747-754. doi:00000478-200506000-00004 [pii]
22. Schrader, A. J., Lechner, O., Templin, M., Dittmar, K. E., Machtens, S., Mengel, M., et al. (2002). CXCR4/CXCL12 expression and signalling in kidney cancer. *British Journal of Cancer*, 86(8), 1250-1256. doi:10.1038/sj.bjc.6600221 [doi]
23. Pan, J., Mestas, J., Burdick, M. D., Phillips, R. J., Thomas, G. V., Reckamp, K., et al. (2006). Stromal derived factor-1 (SDF-1/CXCL12) and CXCR4 in renal cell carcinoma metastasis. *Molecular Cancer*, 5, 56. doi:1476-4598-5-56 [pii]
24. Dahlberg, C. I., Sarhan, D., Chrobok, M., Duru, A. D., & Alici, E. (2015). Natural killer cell-based therapies targeting cancer: Possible strategies to gain and sustain anti-tumor activity. *Frontiers in Immunology*, 6, 605. doi:10.3389/fimmu.2015.00605 [doi]

25. Champsaur, M., & Lanier, L. L. (2010). Effect of NKG2D ligand expression on host immune responses. *Immunological Reviews*, 235(1), 267-285. doi:10.1111/j.0105-2896.2010.00893.x [doi]
26. Gibney, G. T., Aziz, S. A., Camp, R. L., Conrad, P., Schwartz, B. E., Chen, C. R., et al. (2013). c-met is a prognostic marker and potential therapeutic target in clear cell renal cell carcinoma. *Annals of Oncology : Official Journal of the European Society for Medical Oncology*, 24(2), 343-349. doi:10.1093/annonc/mds463 [doi]
27. Truong, L. D., & Shen, S. S. (2011). Immunohistochemical diagnosis of renal neoplasms. *Archives of Pathology & Laboratory Medicine*, 135(1), 92-109. doi:10.1043/2010-0478-RAR.1 [doi]
28. Bailey, A., & McDermott, D. F. (2013). Immune checkpoint inhibitors as novel targets for renal cell carcinoma therapeutics. *Cancer Journal (Sudbury, Mass.)*, 19(4), 348-352. doi:10.1097/PPO.0b013e31829e3153 [doi]
29. Benson, D. M., Jr, Bakan, C. E., Mishra, A., Hofmeister, C. C., Efebera, Y., Becknell, B., et al. (2010). The PD-1/PD-L1 axis modulates the natural killer cell versus multiple myeloma effect: A therapeutic target for CT-011, a novel monoclonal anti-PD-1 antibody. *Blood*, 116(13), 2286-2294. doi:10.1182/blood-2010-02-271874 [doi]
30. Goronzy, J. J., & Weyand, C. M. (2003). Aging, autoimmunity and arthritis: T-cell senescence and contraction of T-cell repertoire diversity - catalysts of autoimmunity and chronic inflammation. *Arthritis Research & Therapy*, 5(5), 225-234. doi:10.1186/ar974 [doi]
31. Ferson, M., Edwards, A., Lind, A., Milton, G. W., & Hersey, P. (1979). Low natural killer-cell activity and immunoglobulin levels associated with smoking in human subjects. *International Journal of Cancer*, 23(5), 603-609.
32. Brodin, P., & Davis, M. M. (2017). Human immune system variation. *Nature Reviews Immunology*, 17(1), 21-29. doi:10.1038/nri.2016.125 [doi]
33. Brodin, P., Jovic, V., Gao, T., Bhattacharya, S., Angel, C. J., Furman, D., et al. (2015). Variation in the human immune system is largely driven by non-heritable influences. *Cell*, 160(1-2), 37-47. doi:10.1016/j.cell.2014.12.020 [doi]